Record Low Antarctic Sea Ice in Austral Winter 2023: Mechanisms and Predictability

Zachary Espinosa[1], Edward Blanchard-Wrigglesworth[1], and Cecilia M. Bitz[1]

[1]Atmospheric Sciences, University of Washington, Seattle, Washington

Key Points:

- An Earth System Model run with historical forcing and nudged to observed winds reproduces the austral winter 2023 sea ice area (SIA) anomaly.
- About 70% of the SIA anomaly is attributable to warm Southern Ocean SSTs that developed prior to 2023 and the remaining ∼30% is attributable to instantaneous atmospheric circulation.
- ENSO conditions in 2023 had a negligible impact on Antarctic sea ice loss in 2023.

Corresponding author: Zachary Espinosa, `zespinos@uw.edu`

Abstract

Since 2016, Antarctic sea ice area (SIA) has set three record summertime minimums occurring in 2017, 2022, and 2023. These recent extremes culminated in a record low SIA anomaly in austral winter 2023, when SIA was over 2 million km^2 below climatology, resulting from negative sea ice concentration (SIC) anomalies centered in the Ross, eastern Weddell, and East Antarctic Seas. We show that a fully-coupled Earth System Model run with historic and anthropogenic forcing and nudged to observed winds over 1950-2023 reproduces the observed austral winter 2023 SIC anomalies. In a sensitivity test that had the impact of 2023 ENSO conditions removed via regression, we show that the 2023 transition from La Niña to El Niño had a negligible impact. Next, using an ensemble initialized on January 1st 2023 nudged to past years' winds, we demonstrate that ∼70% of the total Antarctic SIA anomaly was predictable six months in advance and driven by warm Southern Ocean sea surface temperatures that developed prior to 2023, with the remaining ∼30% attributable to 2023 atmospheric circulation. Finally, an ensemble forecast suggests that Antarctic SIA is likely to remain significantly below climatology in austral winter 2024 due to continuing warm Southern Ocean conditions.

Plain Language Summary

Since 2016, the area of sea ice around Antarctica during summer has reached record low levels three times (in 2017, 2022, and 2023), and the largest negative anomaly by area around Antarctica ever recorded occurred in winter 2023. In our study, we demonstrate that an Earth System model, which considers actual wind patterns and historical forcing, can accurately replicate the observed changes in sea ice concentration during the winter of 2023. Using this framework, we generate a 21-member forecasting ensemble starting on January 1st, 2023, and find that ∼70% of the total sea ice anomaly in Antarctica during the winter could be forecast six months in advance. This predictability is mainly due to warm sea surface temperatures that emerged prior to 2023. Additional simulations suggest that the recent switch from La Niña to El Niño had little effect on the record event. Finally, we generate an ensemble forecast that is initialized on January 1st, 2024 and show that Antarctic sea ice is unlikely to recover to climatology in winter 2024 due to persistently warm Southern Ocean conditions.

1 Introduction

Antarctic sea ice impacts atmosphere-ocean interactions, ocean circulation, marine and coastal ecosystems, ice-sheet and ice-shelf stability, and planetary albedo. Between 1979 and 2015 Antarctic sea ice exhibited a slight increase in sea ice area (SIA), despite the increase in global mean temperature during this time (Comiso et al., 2017). Various mechanisms have been proposed to explain this expansion, including a strengthening Southern Annual Mode due to ozone depletion (Ferreira et al., 2015), changes to southern-ocean freshening via glacial and ice-sheet melt (Dong, Pauling, et al., 2022; Rye et al., 2020; Roach et al., 2023), an increase in precipitation (Liu & Curry, 2010), wind circulation (Blanchard-Wrigglesworth et al., 2021) and wind-driven sea ice transport (Haumann et al., 2016; Sun & Eisenman, 2021), tropically-driven circulation trends (Chung et al., 2022), and internal variability of ocean convection (L. Zhang et al., 2019). Complicating our ability to study the expansion of Antarctic SIA is the fact that most state-of-the-art Earth System Models (ESMs) when run with historical and anthropogenic forcing simulate a loss in Antarctic SIA over the satellite era (Roach et al., 2020).

Despite the increase in SIA over 1979-2015, Antarctica has experienced a reversal in sea ice trends since 2016 (Parkinson, 2019; Purich & Doddridge, 2023), a rapidly warming Southern Ocean (Meehl et al., 2019; Wilson et al., 2023) and a sequence of extraordinary atmospheric heatwaves (Blanchard-Wrigglesworth et al., 2023; Gorodetskaya et al., 2023; Wille et al., 2024). The reversal first began in September 2016 and developed into a record areal anomaly in austral spring and record-minimum in February 2017 (Turner et al., 2017). Factors contributing to this event include a near-record negative Southern Annual Mode (SAM), warm Southern Ocean sea surface temperatures (SSTs), and a zonal wave 3 pattern of atmospheric circulation in early winter. These local conditions have been linked to the negative trend in the Interdecadal Pacific Oscillation (IPO) (Meehl et al., 2019), an extreme El Niño in 2015/2016 (Stuecker et al., 2017), and variability in the polar stratospheric vortex (Wang et al., 2019). After a slight recovery in the intervening years, a new record sea ice extent (SIE) minimum occurred in February 2022, when SIE dropped to 1.97 million km^2 (Raphael & Handcock, 2022; C. Zhang & Li, 2023; Turner et al., 2022). Only one year later, in February 2023 this record was broken with a new summer SIE minimum of 1.79 million km^2 (Cordero et al., 2023). Several studies have examined the impact of a strongly positive SAM, La Niña conditions, and variability in the Amundsen Sea Low on sea ice minimums in February 2022 and 2023 (C. Zhang & Li, 2023; Turner et al., 2022; Cordero et al., 2023). Throughout the remainder of 2023 negative SIA anomalies dramatically amplified and by the austral winter SIA anomalies were over 2 million km^2 below climatology, an anomaly of over 5 sigma units, and .9 million km^2 lower than the previous largest negative seasonal SIA anomaly (Figure 1A).

A growing body of literature has emerged using atmospheric nudging in ESMs, in which zonal and meridional winds are relaxed to reanalysis, to develop a process understanding of Antarctic sea ice variability and trends (Blanchard-Wrigglesworth et al., 2021; Roach et al., 2023) and Southern Ocean SST variability (Dong, Armour, et al., 2022). We find that a state-of-the-art Earth System Model run between 1950 and 2023 with historical forcing and nudged to winds from reanalysis successfully reproduces the observed pattern and magnitude of sea ice concentration anomalies in austral winter, 2023. Using this wind-nudging framework, we then conduct several experiments in order to decompose the event's drivers: (1) we generate a 21-member ensemble forecast initialized on January 1st, 2023 to show that ∼70% of the total SIA anomaly is attributable to warm Southern Ocean SSTs that developed by the end of 2022 and offered significant predictability at a six month lead; (2) we demonstrate that the transition from La Niña to El Niño in 2023 had a negligible impact on SIA anomalies by removing the linear impact of 2023 ENSO conditions from atmospheric winds and re-nudging to 'ENSO-less' winds; (3) we demonstrate, using an ensemble forecast, that Antarctic SIA is likely to remain near record lows in winter 2024.

2 Methods

2.1 Observations, Reanalysis, and Indices

Simulations are evaluated with satellite-derived passive microwave measurements of sea ice concentrations (SIC) in the Southern Ocean (SO) from the NSIDC Climate Data Record version 4 on a 25km x 25km polar stereographic grid (Meier & Stewart., 2021), and ERA5 reanalysis for all other atmospheric and oceanic conditions (Hersbach et al., 2020). All data are regridded to a common 1° global resolution before analysis. All subsequent analysis of sea ice coverage is reported in sea ice area (SIA), rather than sea ice extent (SIE) (Matthews et al., 2020), because Antarctic wintertime sea ice does not suffer data quality issues such as a 'pole hole' or significant melt pond coverage that in the Arctic justify the use of SIE.

We calculate the Amundsen Sea Low location (latitude and longitude) and central pressure between January 1979 and August 2023 following Hosking et al. (2016). The Niño3.4 time series that we use is from `https://psl.noaa.gov/data/correlation/nina34.data`. We calculate the Southern Annual Mode (SAM) index following Marshall (2003).

2.2 Nudging CESM2.1 to Historical Winds

We use the Community Earth System Model version 2.1 (CESM2.1) from the National Center for Atmospheric Research with the Community Atmosphere Model version 6 (CAM6) (Danabasoglu et al., 2020). Simulations are forced with CMIP6 historical forcing through 2014 and thereafter with SSP3.7 forcing. All components have a nominal 1° resolution. Model output is regridded to the same grid as used for reanalysis and observations.

In all nudging simulations (Table S1), we nudge zonal (U) and meridional (V) winds to 6-hourly ERA5 U and V from 850hPa to the top of the model between 55°S and 80°S following the methodology described in Blanchard-Wrigglesworth et al. (2021). The wind-nudging is performed by relaxing the winds as follows:

$$\frac{dx}{dt} = F(x) + F_{nudge}$$

$$F_{nudge} = \frac{\alpha[x_T(t_{next}) - x(t)]}{t_{next} - t}$$

where x is the model state-vector being nudged (i.e. U or V), $F(x)$ is the model-calculated tendency of x, and F_{nudge} is the relaxation tendency, which is proportional to the difference between $x_T(t_{next})$, the target state-vector at the next time step, and $x(t)$, the model state-vector at the current time-step. α is the nudging coefficient which is set to 1 between 55°S and 80°S and smoothly transitions to 0 outside of the nudging domain border. CESM2-NUDGE requires approximately 30-years to adjust to a stable Antarctic sea ice state (Figure S1). For this reason, nudging is initiated in 1950 and all model output prior to 1980 is rejected from analysis.

Our baseline simulation, initialized on January 1, 1950, and integrated through December 31, 2023, is henceforth denoted as CESM2-NUDGE (Table S1).

2.3 Nudging CESM2.1 to 'ENSO-less' 2023 winds

An additional nudging simulation branches from CESM2-NUDGE on January 1st, 2023 and is nudged to adjusted observed winds over January 1 2023 - August 31 2023 where the observed linear relationship between Niño 3.4 and U and V is removed. In this experiment the target wind anomalies are updated as follows:

$$x'_{T,NO-ENSO}(t) = x'_T(t) - \frac{dx'_T}{dNino3.4'} Nino3.4'(t)$$

where $x'_T(t)$ is the anomaly target state-vector at time t, $\frac{dx'_T}{dNino3.4'}$ is the instantaneous daily regression coefficient between the time series of Niño3.4 anomalies and target state-vector anomalies, and $Nino3.4'(t)$ is the Niño3.4 anomaly at the target time t. The updated target state-vector anomaly with the linear impact of ENSO removed, $x'_{T,NO-ENSO}(t)$, is then added to $\overline{x_T}$, the daily climatology of the target state-vector. Regression coefficients are calculated using monthly time series of the $Nino3.4'(t)$ index and target state-vector and are linearly interpolated to a daily resolution. Regression coefficients and all anomalies are calculated using a reference period between January 1, 1980 and December 31, 2022. The simulation that is nudged to historical winds with ENSO removed is henceforth denoted as CESM2-NO-ENSO-NUDGE (Table S1).

2.4 Reforecasting the Austral Winter 2023 by Nudging CESM2.1

In order to examine the predictability of the winter 2023 Antarctic SIA anomaly and further understand its mechanisms, we generate a 21-member forecast ensemble initialized from CESM2-NUDGE on January 1, 2023, and run for a year. In order to sample different atmospheric conditions, each ensemble member is nudged to target winds taken from a random year between 1979 and 2022 (Table S1). We nudge to winds from previous years rather than allowing the ensemble members to free-run in order to estimate the predictability of the winter 2023 SIA anomaly without the influence of climate drift. A similar sea ice forecast technique is used by ice-ocean models that use past years' atmospheric boundary conditions to evolve the model forwards (e.g., Lindsay et al. (2012)). Model simulations that are nudged to historical winds from past years are henceforth referred to as CESM2-REFORECAST-2023. We consider these experiments 'forecasts' because they could have been generated on January 1st, 2023, i.e., at least six months before austral winter 2023.

2.5 Forecasting the Austral Winter 2024 by Nudging CESM2.1

Finally, the skillful results of CESM2-REFORECAST-2023 encourage us to generate a sea ice forecast for austral winter 2024. Will winter SIA in 2024 rebound to the pre-2020s climatology or will it remain anomalously low? Like the 2023 forecast, we generate a 22-member ensemble initialized from CESM2-NUDGE on January 1, 2024. Each ensemble member runs until December 31, 2024 and is nudged to past winds taken from the same random years as CESM2-REFORECAST-2023, with an additional ensemble member that is nudged to winds from 2023, in order to further examine the impact of the atmospheric circulation in 2023 in driving SIA anomalies. These experiments are henceforth referred to as CESM2-FORECAST-2024.

3 Results

3.1 Conditions leading to sea ice loss in Austral Winter 2023

The SIA in austral winter (June, July and August; JJA) 2023 was 11.5 million km^2 and 2.2 million km^2 below the 1980-2020 climatology, representing a 5-sigma event and the largest negative areal anomaly on record (Figure 1A). Negative SIC anomalies were observed in all regions of the SO except for the Amundsen-Bellingshausen Sea, which exhibited a positive SIA anomaly of .2 million km^2 (Figure 1B). The most pronounced negative anomalies occurred in the Ross, Weddell, and South Indian Seas, at .7 million km^2, .74 million km^2, and .73 million km^2, respectively (Figure 1H). These regional anomalies were extreme, representing -3.0, -2.4, and -3.2 sigma events, respectively (Figure S2). The large scale atmospheric circulation in JJA 2023 was dominated by large positive sea level pressure (SLP) anomalies in the Ross Sea and zonally characterized by a wave three pattern, with weaker positive SLP anomalies over the East Weddell and South Indian Seas (Figure 1F). The associated anomalous anticyclonic circulation drove northward sea ice motion and cold air advection leading to positive anomalies in the Bellingshausen Sea and southward sea ice motion and warm air advection in the Eastern Ross and Weddell Seas (Figure 2E). Past studies have shown that the impact of the zonal wave three pattern is greatest during the growth season (Raphael, 2007), when sea ice expansion is rapid and sensitive to warm-air advection and trends in winter meridional winds can help explain trends in winter SIC (Blanchard-Wrigglesworth et al., 2021). Dynamically driven anomalies may have been amplified or counteracted by warm ocean surface conditions, which can inhibit lateral and basal growth. For example, the Eastern Weddell Sea is characterized by negative SIC anomalies despite southerly surface-winds at the ice-edge (along longitudes 20W-30E in Fig 2E/F) that would typically be associated with a northward expansion of the wintertime ice-edge. The pattern of SST anomalies matches the pattern of SIC anomalies in every sector (Figure 1D). Warm SO surface conditions emerged as early as summer 2017 (Figure 2A) and suggest the role of preconditioning and possible seasonal predictability (see below in Section 3.3).

3.2 Reconstructing sea ice loss in a global climate model

Having examined the atmospheric and oceanic conditions during austral winter 2023, we turn our attention to decomposing the relative contribution of potential drivers by analyzing the nudged simulations with CESM2. CESM2-NUDGE generates SIC anomalies for winter 2023 of the same magnitude and pattern as observations (Figure 1B and 1C). The CESM2-NUDGE SIA in JJA 2023 is 2.45 million km^2 below the model-defined 1980-2020 climatology, with regional SIA anomalies comparable to those in observations (Figure 1H and 1I). Additionally, the spatial pattern of SST anomalies is similar to observations, albeit with a slight positive circumpolar bias. The remarkable similarity between SIC and SST anomalies in CESM2-NUDGE and observations suggests processes connect these quantities, possibly causally. Nudging in CESM2 is a powerful tool for disentangling the relevant drivers of this record event.

To begin, the temporal evolution of SO SST anomalies generated in CESM2-NUDGE are similar to observations, with circumpolar warm SSTs first emerging in austral summer 2017 and persisting until present day (Figure 2A and 2B). The similarity of SST variability in CESM2-NUDGE and observations (Figure 2A and 2B) suggests that the recent emergence of warm surface ocean conditions may have been driven, in part, by surface wind-stress. Similar to observations, meridional near-surface winds at the ice-edge associated with the zonal-wave three pattern explain to a large degree SIC anomalies about the zonal mean in JJA 2023 (Figure 2F). Differences between observations and CESM2-NUDGE (Figure 2E and 2F) may be a result of differences in the position of the JJA 2023 ice-edge (Figure 1B and 1C). We can further decompose the drivers of SIC anomalies by examining the spatial pattern of ice-area change over time (i.e. ice-area tendency), which is the sum of thermodynamic and dynamic terms:

$$\frac{dA}{dt} = \left(\frac{dA}{dt}\right)_{thermodynamic} + \left(\frac{dA}{dt}\right)_{dynamic}$$

, where the dynamic contribution is driven by advection and deformation of the ice-pack and the thermodynamic contribution is driven by melt and growth processes. The spatially averaged total ice-area tendency is anomalously low during the growth season (March - August) 2023 and dominated by thermodynamic contributions (Figure S3G). Monthly thermodynamic ice-area tendencies are negative starting in March 2023 and remain anomalously low throughout August 2023 as the sea ice edge expands into warm SO SSTs. The spatial pattern of thermodynamic contributions is characterized by negative anomalies within the ice edge in all sectors of the SO except the Bellingshausen Sea. Dynamic contributions to ice-area changes are dominated by wind-driven sea ice advection, with positive contributions south of the ice-edge and negative contributions north of the ice-edge (Figure S3B). Despite the spatially averaged dynamic contribution being slightly positive during much of the growth season, dynamic tendency anomalies explain negative SIC anomalies in the Ross, Bellingshausen and Weddell Seas.

3.3 The Impact of 2023 ENSO conditions on sea ice loss

Next, we turn our attention to the impact of 2023 ENSO conditions on Antarctic sea ice in austral winter 2023. La Niña conditions first emerged in spring 2020, peaked in early 2021, and persisted until early 2023 when ENSO transitioned to an El Niño phase in March 2023 which steadily amplified throughout 2023 (Figure S4). It is well known that ENSO events can generate stationary Rossby Waves and influence SO atmospheric circulation and SIC (Li et al., 2021). Here, we calculate the linear impact of 2023 ENSO conditions on SO conditions as the residual between CESM2-NUDGE and CESM2-NO-ENSO-NUDGE. 2023 ENSO conditions slightly amplified negative anomalies in the Ross and Weddell Seas and positive anomalies in the Bellingshausen Sea (Figure 3). Although the impact of the transition from La Niña to El Niño on sea ice is consistent with past literature (Li et al., 2021), the total contribution is only about .06 million km^2 of the total 2.45 million km^2 SIA anomaly, amounting to roughly 3% of the total anomaly in CESM2-NUDGE. The transition to El Niño acted to weaken the ASL by about 5 hPa in the Ross sea (e.g. amplify positive SLP anomalies in the Ross Sea), which amplified anomalous anticyclonic circulation and strengthened northward and southward sea ice advection in the Bellingshausen and Ross Seas, respectively (Figure 3C). In the Weddell sector, 2023 ENSO conditions amplified northerly surface winds, which contributed to a southward shift in the sea ice edge (Figure 3A). We validate the results presented here with those derived from a composite analysis from CESM2-NUDGE of all periods with a positive (El Niño) or negative (La Niña) anomaly in the observed JJA Niño3.4 index greater than 1-standard deviation between 1979 and 2022 (Figure S5). We find that the fingerprint of ENSO on SO conditions are consistent between nudging simulation (Figure 3) and composite results (Figure S5), albeit weaker in 2023, likely because 2023 ENSO conditions where neutral in early 2023.

3.4 The relative importance of atmosphere and ocean forcing

The emergence of warm ocean conditions prior to 2023 may be associated with persistent La Niña conditions between 2020 and 2023 (Figure S4), deepening of the ASL (Figure S4), and enhanced upwelling warm waters from below the mixed layer. While the exact cause for a warmer SO state is beyond the scope of this study, the ability of CESM2-NUDGE to reproduce the timing and magnitude of SST anomalies since 2017 by nudging zonal and meridional winds to reanalysis suggests that atmospheric circulation anomalies are a critical component of recent trends (Figure 2A and 2B). Previous studies have suggested that warm SO subsurface conditions influenced SSTs via wind-driven mixing and that warm SO SSTs have been essential in driving recent Antarctic sea ice lows (L. Zhang et al., 2022). Purich and Doddridge (2023) further argue that SO subsurface warming since 2017 may have driven Antarctic sea ice cover into a persistent low state. In agreement with these trends, CESM2-NUDGE exhibits anomalously deep mixed-layer-depth throughout the SO in JJA 2023, suggesting enhanced SO surface-subsurface mixing (Figure S8). The emergence of warm SST anomalies prior to 2023 further suggests that a substantial fraction of the austral winter sea ice anomaly may have been predictable several months in advance, as SST anomalies can provide significant predictive skill for sea ice (Holland et al., 2013). In addition, as noted above, winter 2023 SIC anomalies were negative in some regions that had southerly wind anomalies during winter 2023. Southerly wind anomalies would themselves promote positive rather than negative SIC anomalies, implying a significant role for ocean conditions in driving winter 2023 SIC anomalies.

The CESM2-REFORECAST-2023 ensemble-mean reproduces a strong negative SIA winter 2023 anomaly that is about ∼70% of the total JJA 2023 anomaly simulated in CESM2-NUDGE (-1.8 million km^2 vs -2.5 million km^2 in CESM2-Nudge, Figure 4) despite nudging the ensemble members to winds from a year other than 2023 (i.e., drawn from 1980-2022). From this result we conclude that about ∼70% of the total JJA SIA anomaly is preconditioned by the initialized anomalies in the ice-ocean on January 1 2023, which themselves may be partly attributable to atmospheric forcing prior to 2023 (Figure 4A). The remaining ∼30% of the total JJA 2023 anomaly (the residual or forecast error) can be attributed to atmospheric forcing during 2023 (Figure S7). Hovmoller diagrams reveal the dominant role SO SSTs played in driving the ensemble-mean SIA anomaly, as SST remained anomalously warm in CESM2-REFORECAST-2023, albeit slightly weaker than in CESM2-NUDGE (Figure 4C), played in driving the ensemble-mean SIA anomaly. A regional decomposition of the SIA forecast error also reveals that atmospheric forcing during 2023 had the largest impact in the Ross and Bellingshausen sectors (Figure 4I and Figure 4J), where enhanced cyclonic circulation and the resultant sea ice advection drove a large fraction of the anomalies, consistent with the largest SLP anomalies in winter 2023 being located in the Ross and Bellingshausen sectors (Figure 1). This decomposition confirms the multifactorial drivers that contributed to the record low Antarctic SIA in austral winter 2023.

3.5 Forecasting 2024 austral winter sea ice conditions

Given the importance of SO SSTs in driving the record JJA 2023 SIA anomaly and the persistence of warm SO SSTs throughout 2023 (Figure S9), we hypothesise that SIA is likely to remain below climatology in JJA 2024. In order to examine this, we generate a forecast for 2024 initialized from CESM2-NUDGE. All 22-ensemble members in the CESM2-FORECAST-2024 ensemble forecast a negative wintertime SIA anomaly (Figure S13-14), with a forecast range of -1.8 million to -2.6 million km^2, and a forecast mean of -2.15 million km^2 (Figure 5). The ensemble-mean forecast exhibits negative SIA anomalies in all sectors of the SO (Figure 5), with the largest ensemble spread in the Weddell sector. In fact, the ensemble-mean SIA forecast for JJA 2024 is roughly .35 million km^2 more negative than the ensemble-mean forecast for JJA 2023 generated by CESM2-REFORECAST-2023. This may result from the fact that warm SST anomalies in the SO, which were already anomalously warm by the end of 2022, have amplified throughout 2023 (Figure S9). Finally, if the atmospheric circulation that occurred in 2023 repeated itself in 2024, we find that SIA in JJA 2024 would be 2.6 million km^2 below climatology, which is the lowest SIA forecast within the CESM2-FORECAST-2024 ensemble, and more negative than the record CESM2-NUDGE anomaly in JJA 2023, consistent with our finding that winds from 2023 amplified the SIA anomalies in 2023.

4 Conclusions

The largest recorded negative Antarctic SIA anomaly in the satellite era occurred in austral winter 2023. The record sea ice conditions resulted from the combination of a fast response to anomalous atmospheric circulation forcing in 2023 and a slower, lagged response to ocean SST anomalies that emerged prior to 2023. The event had significant predictability at a six-to-eight month leadtime, was weakly impacted by 2023 ENSO conditions, and is likely to persist into winter 2024.

The tools presented here are a novel use of the circulation nudging framework in a fully coupled model. We demonstrate that these techniques can be used to study the impact of large-scale modes of variability (e.g. ENSO) on remote conditions (e.g. Antarctic sea ice) by removing via regression the relationship between the target variable and mode of interest. The application of the atmospheric wind nudging framework as a tool for studying seasonal sea ice predictability also paves the way for further development of sea ice forecasting systems, which for Antarctic sea ice have historically shown poor skill at seasonal timescales (Massonnet et al., 2023).

Several studies have argued that the reversal of Antarctic SIA trends and the warming in the SO is indicative of a regime-shift into a new, low Antarctic sea ice mean-state. (Purich & Doddridge, 2023; Schroeter et al., 2023; Eayrs et al., 2021). While it is likely too soon to robustly determine a permanent regime-shift, our forecast that Antarctic sea ice is likely to remain near record lows in winter 2024 builds upon this concern and highlights the need for further investigation into SO surface and subsurface temperature variability, and to further understand the attribution of recent SO warming - is it due to internal variability or early signs of a forced warming response?

Data Availability

ERA5 reanalysis (Hersbach et al., 2020) are available at `https://www.ecmwf.int/en/forecasts/dataset/ecmwf-reanalysis-v5`. Raw data generated from CESM2.1 model experiments available upon request. Satellite derived passive microwave measurements of sea ice concentrations from the NSIDC Climate Data Record version 4 on a 25km x 25km polar stereographic grid (Meier & Stewart., 2021) are available at `https://nsidc.org/data/g02202/versions/4`. Code used to generate the Amundsen Sea low location and pressure can be found at `https://github.com/scotthosking/amundsen-sea-low-index/`. The Niño3.4 timeseries can be found at `https://psl.noaa.gov/data/correlation/nina34.data`, and the Southern Annual Mode index Marshall (2003) is available at `https://legacy.bas.ac.uk/met/gjma/sam.html`. Instructions to run CESM2.1 simulations can be found at `https://escomp.github.io/CESM/versions/cesm2.1/html/downloading_cesm.html`.

Code Availability

The code used for all analyses presented in this manuscript is publicly available at `https://github.com/zacespinosa/SI-Antarctic`.

Acknowledgments

ZE would like to thank the following software communities for making their software publicly available: xsearch (`https://github.com/pochedls/xsearch`), xarrays (`https://docs.xarray.dev/en/stable/`), xskillscore (`https://xskillscore.readthedocs.io/en/stable/index.html`), SciPy (`https://scipy.org/`), and xCDAT (`https://xcdat.readthedocs.io/en/latest/index.html`). CMB is supported by the National Science Foundation OPP-2237964. ZE is supported by the U.S. Department of Energy, Office of Science, Office of Advanced Scientific Computing Research, Department of Energy Computational Science Graduate Fellowship under Award Number(s) DE-SC0023112. This report was prepared as an account of work sponsored by an agency of the United States Government. Neither the United States Government nor any agency thereof, nor any of their employees, makes any warranty, express or implied, or assumes any legal liability or responsibility for the accuracy, completeness, or usefulness of any information, apparatus, product, or process disclosed, or represents that its use would not infringe privately owned rights. Reference herein to any specific commercial product, process, or service by trade name, trademark, manufacturer, or otherwise does not necessarily constitute or imply its endorsement, recommendation, or favoring by the United States Government or any agency thereof. The views and opinions of authors expressed herein do not necessarily state or reflect those of the United States Government or any agency thereof. This work uses ERA5 data, which contains modified Copernicus Climate Change Service information 2020. Neither the European Commission nor ECMWF is responsible for any use that may be made of the Copernicus information or data it contains. We would also like to acknowledge high-performance computing support from Cheyenne (https://doi.org/10.5065/D6RX99HX) provided by NCAR's Computational and Information Systems Laboratory, sponsored by the National Science Foundation.

References

Blanchard-Wrigglesworth, E., Roach, L. A., Donohoe, A., & Ding, Q. (2021, February). Impact of Winds and Southern Ocean SSTs on Antarctic Sea Ice Trends and Variability. *Journal of Climate*, *34*(3), 949–965. doi: 10.1175/JCLI-D-20-0386.1

Blanchard-Wrigglesworth, E., Cox, T., Espinosa, Z. I., & Donohoe, A. (2023). The largest ever recorded heatwave—characteristics and attribution of the antarctic heatwave of march 2022. *Geophysical Research Letters*, *50*(17), e2023GL104910.

Chung, E.-S., Kim, S.-J., Timmermann, A., Ha, K.-J., Lee, S.-K., Stuecker, M. F., ... Huang, L. (2022, May). Antarctic sea-ice expansion and Southern Ocean cooling linked to tropical variability. *Nature Climate Change*, *12*(5), 461–468. doi: 10.1038/s41558-022-01339-z

Comiso, J. C., Gersten, R. A., Stock, L. V., Turner, J., Perez, G. J., & Cho, K. (2017, March). Positive Trend in the Antarctic Sea Ice Cover and Associated Changes in Surface Temperature. *Journal of Climate*, *30*(6), 2251–2267. doi: 10.1175/JCLI-D-16-0408.1

Cordero, R. R., Feron, S., Damiani, A., Llanillo, P. J., Carrasco, J., Khan, A. L., ... Casassa, G. (2023). Signature of the stratosphere-troposphere coupling on recent record-breaking antarctic sea ice anomalies. *The Cryosphere Discussions*, *2023*, 1–20.

Danabasoglu, G., Lamarque, J.-F., Bacmeister, J., Bailey, D., DuVivier, A., Edwards, J., ... others (2020). The community earth system model version 2 (cesm2). *Journal of Advances in Modeling Earth Systems*, *12*(2), e2019MS001916.

Dong, Y., Armour, K. C., Battisti, D. S., & Blanchard-Wrigglesworth, E. (2022). Two-way teleconnections between the southern ocean and the tropical pacific via a dynamic feedback. *Journal of Climate*, *35*(19), 6267–6282.

Dong, Y., Pauling, A. G., Sadai, S., & Armour, K. C. (2022). Antarctic Ice-Sheet

Meltwater Reduces Transient Warming and Climate Sensitivity Through the Sea-Surface Temperature Pattern Effect. *Geophysical Research Letters*, *49*(24), e2022GL101249. doi: 10.1029/2022GL101249

Eayrs, C., Li, X., Raphael, M. N., & Holland, D. M. (2021, July). Rapid decline in Antarctic sea ice in recent years hints at future change. *Nature Geoscience*, *14*(7), 460–464. doi: 10.1038/s41561-021-00768-3

Ferreira, D., Marshall, J., Bitz, C. M., Solomon, S., & Plumb, A. (2015, February). Antarctic Ocean and Sea Ice Response to Ozone Depletion: A Two-Time-Scale Problem. *Journal of Climate*, *28*(3), 1206–1226. doi: 10.1175/JCLI-D-14-00313.1

Gorodetskaya, I., Durán-Alarcón, C., Gonzalez-Herrero, S., Clem, K., imazio, p. r., Santos, C. L.-D., ... others (2023). Compound drivers behind new record high temperatures and surface melt at the antarctic peninsula in february 2022.

Haumann, F. A., Gruber, N., Münnich, M., Frenger, I., & Kern, S. (2016, September). Sea-ice transport driving Southern Ocean salinity and its recent trends. *Nature*, *537*(7618), 89–92. doi: 10.1038/nature19101

Hersbach, H., Bell, B., Berrisford, P., Hirahara, S., Horányi, A., Muñoz-Sabater, J., ... others (2020). The era5 global reanalysis. *Quarterly Journal of the Royal Meteorological Society*, *146*(730), 1999–2049.

Holland, M. M., Blanchard-Wrigglesworth, E., Kay, J., & Vavrus, S. (2013). Initial-value predictability of antarctic sea ice in the community climate system model 3. *Geophysical Research Letters*, *40*(10), 2121–2124.

Hosking, J. S., Orr, A., Bracegirdle, T. J., & Turner, J. (2016). Future circulation changes off west antarctica: Sensitivity of the amundsen sea low to projected anthropogenic forcing. *Geophysical Research Letters*, *43*(1), 367–376.

Li, X., Cai, W., Meehl, G. A., Chen, D., Yuan, X., Raphael, M., ... Song, C. (2021, October). Tropical teleconnection impacts on Antarctic climate changes. *Nature Reviews Earth & Environment*, *2*(10), 680–698. doi: 10.1038/s43017-021-00204-5

Lindsay, R., Haas, C., Hendricks, S., Hunkeler, P., Kurtz, N., Paden, J., ... Zhang, J. (2012). Seasonal forecasts of arctic sea ice initialized with observations of ice thickness. *Geophysical research letters*, *39*(21).

Liu, J., & Curry, J. A. (2010, August). Accelerated warming of the Southern Ocean and its impacts on the hydrological cycle and sea ice. *Proceedings of the National Academy of Sciences*, *107*(34), 14987–14992. doi: 10.1073/pnas.1003336107

Marshall, G. J. (2003). Trends in the southern annular mode from observations and reanalyses. *Journal of climate*, *16*(24), 4134–4143.

Massonnet, F., Barreira, S., Barthélemy, A., Bilbao, R., Blanchard-Wrigglesworth, E., Blockley, E., ... others (2023). Sipn south: six years of coordinated seasonal antarctic sea ice predictions. *Frontiers in Marine Science*, *10*, 1148899.

Matthews, J. L., Peng, G., Meier, W. N., & Brown, O. (2020). Sensitivity of arctic sea ice extent to sea ice concentration threshold choice and its implication to ice coverage decadal trends and statistical projections. *Remote Sensing*, *12*(5), 807.

Meehl, G. A., Arblaster, J. M., Chung, C. T. Y., Holland, M. M., DuVivier, A., Thompson, L., ... Bitz, C. M. (2019, December). Sustained ocean changes contributed to sudden Antarctic sea ice retreat in late 2016. *Nature Communications*, *10*(1), 14. doi: 10.1038/s41467-018-07865-9

Meier, F. F. A. K. W., W. N., & Stewart., J. S. (2021). *Noaa/nsidc climate data record of passive microwave sea ice concentration, version 4.* National Snow and Ice Data Center. Retrieved from `https://nsidc.org/data/G02202/versions/4` doi: 10.7265/efmz-2t65

Parkinson, C. L. (2019, July). A 40-y record reveals gradual Antarctic sea ice increases followed by decreases at rates far exceeding the rates seen in the Arctic. *Proceedings of the National Academy of Sciences*, *116*(29), 14414–14423. doi: 10.1073/pnas.1906556116

Purich, A., & Doddridge, E. W. (2023, September). Record low Antarctic sea ice coverage indicates a new sea ice state. *Communications Earth & Environment*, *4*(1), 1–9. doi: 10.1038/s43247-023-00961-9

Raphael, M. N. (2007). The influence of atmospheric zonal wave three on Antarctic sea ice variability. *Journal of Geophysical Research: Atmospheres*, *112*(D12). doi: 10.1029/2006JD007852

Raphael, M. N., & Handcock, M. S. (2022, April). A new record minimum for Antarctic sea ice. *Nature Reviews Earth & Environment*, *3*(4), 215–216. doi: 10.1038/s43017-022-00281-0

Roach, L. A., Dörr, J., Holmes, C. R., Massonnet, F., Blockley, E. W., Notz, D., ... Bitz, C. M. (2020, May). Antarctic Sea Ice Area in CMIP6. *Geophysical Research Letters*, *47*(9). doi: 10.1029/2019GL086729

Roach, L. A., Mankoff, K. D., Romanou, A., Blanchard-Wrigglesworth, E., Haine, T. W., & Schmidt, G. A. (2023). Winds and meltwater together lead to southern ocean surface cooling and sea ice expansion. *Geophysical Research Letters*, *50*(24), e2023GL105948.

Rye, C. D., Marshall, J., Kelley, M., Russell, G., Nazarenko, L. S., Kostov, Y., ... Hansen, J. (2020). Antarctic Glacial Melt as a Driver of Recent Southern Ocean Climate Trends. *Geophysical Research Letters*, *47*(11), e2019GL086892. doi: 10.1029/2019GL086892

Schroeter, S., O'Kane, T. J., & Sandery, P. A. (2023, February). Antarctic sea ice regime shift associated with decreasing zonal symmetry in the Southern Annular Mode. *The Cryosphere*, *17*(2), 701–717. doi: 10.5194/tc-17-701-2023

Stuecker, M. F., Bitz, C. M., & Armour, K. C. (2017, September). Conditions leading to the unprecedented low Antarctic sea ice extent during the 2016 austral spring season: RECORD LOW 2016 ANTARCTIC SEA ICE EXTENT. *Geophysical Research Letters*, *44*(17), 9008–9019. doi: 10.1002/2017GL074691

Sun, S., & Eisenman, I. (2021, February). Observed Antarctic sea ice expansion reproduced in a climate model after correcting biases in sea ice drift velocity. *Nature Communications*, *12*(1), 1060. doi: 10.1038/s41467-021-21412-z

Turner, J., Holmes, C., Caton Harrison, T., Phillips, T., Jena, B., Reeves-Francois, T., ... Bajish, C. C. (2022). Record Low Antarctic Sea Ice Cover in February 2022. *Geophysical Research Letters*, *49*(12), e2022GL098904. doi: 10.1029/2022GL098904

Turner, J., Phillips, T., Marshall, G. J., Hosking, J. S., Pope, J. O., Bracegirdle, T. J., & Deb, P. (2017). Unprecedented springtime retreat of Antarctic sea ice in 2016. *Geophysical Research Letters*, *44*(13), 6868–6875. doi: 10.1002/2017GL073656

Wang, G., Hendon, H. H., Arblaster, J. M., Lim, E.-P., Abhik, S., & van Rensch, P. (2019, January). Compounding tropical and stratospheric forcing of the record low Antarctic sea-ice in 2016. *Nature Communications*, *10*(1), 13. doi: 10.1038/s41467-018-07689-7

Wille, J. D., Alexander, S. P., Amory, C., Baiman, R., Barthélemy, L., Bergstrom, D. M., ... others (2024). The extraordinary march 2022 east antarctica "heat" wave. part i: observations and meteorological drivers. *Journal of Climate*, *37*(3), 757–778.

Wilson, E. A., Bonan, D. B., Thompson, A. F., Armstrong, N., & Riser, S. C. (2023, September). Mechanisms for Abrupt Summertime Circumpolar Surface Warming in the Southern Ocean. *Journal of Climate*, *36*(20), 7025–7039. doi: 10.1175/JCLI-D-22-0501.1

Zhang, C., & Li, S. (2023, March). Causes of the record-low Antarctic sea-ice in austral summer 2022. *Atmospheric and Oceanic Science Letters*, 100353. doi: 10.1016/j.aosl.2023.100353

Zhang, L., Delworth, T. L., Cooke, W., & Yang, X. (2019, January). Natural variability of Southern Ocean convection as a driver of observed climate trends. *Nature Climate Change*, *9*(1), 59–65. doi: 10.1038/s41558-018-0350-3

Zhang, L., Delworth, T. L., Yang, X., Zeng, F., Lu, F., Morioka, Y., & Bushuk, M. (2022, November). The relative role of the subsurface Southern Ocean in driving negative Antarctic Sea ice extent anomalies in 2016–2021. *Communications Earth & Environment*, *3*(1), 1–9. doi: 10.1038/s43247-022-00624-1

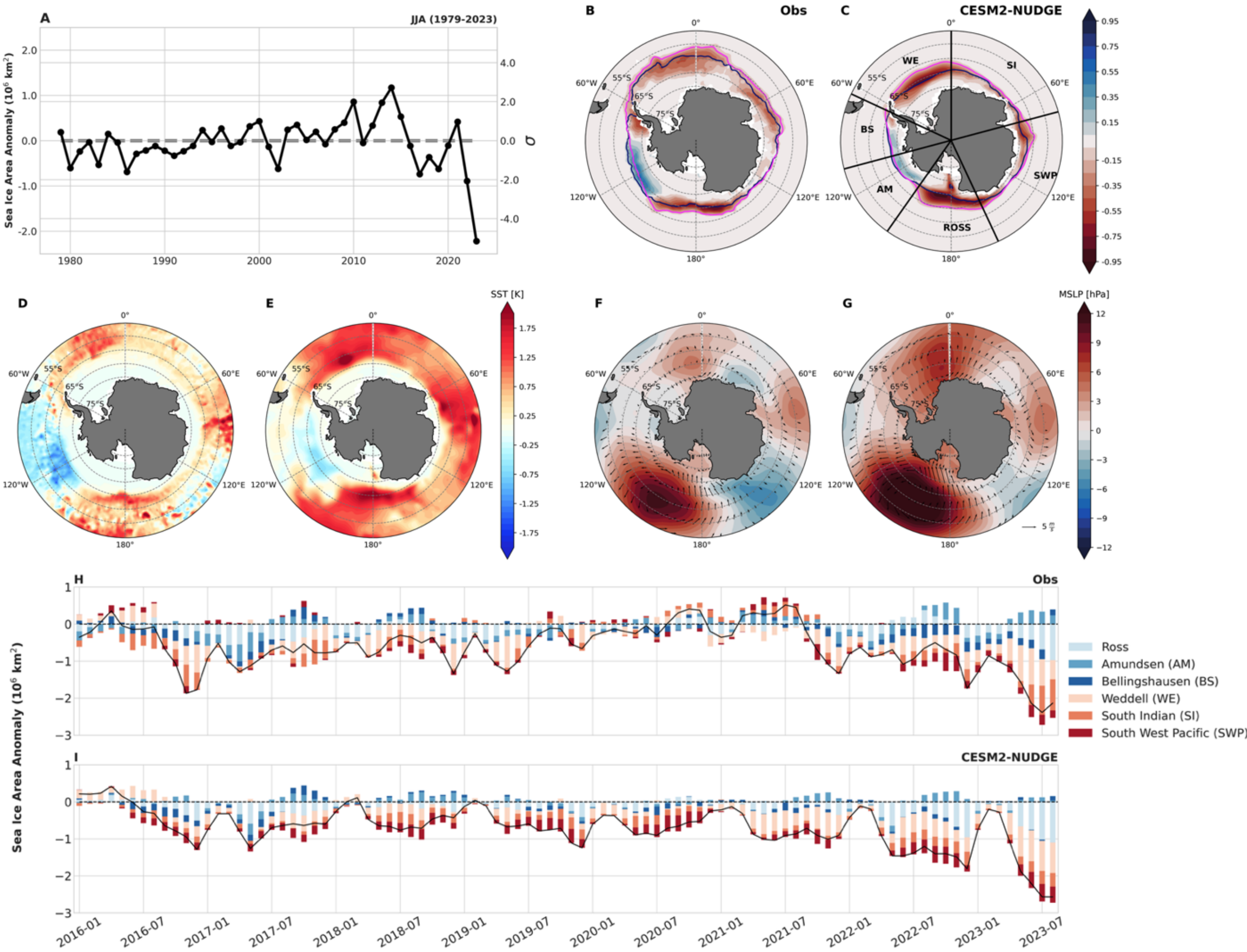

Figure 1. Times series of observed June, July, and August (JJA) raw (million km^2; left) and standardized (σ; right) SIA anomalies between 1979 and 2023 (A). Mean SIC anomalies in JJA 2023 in observations (B) and CESM2-NUDGE (C). Magenta and black contours indicate climatological average (1980-2020) and JJA 2023 sea ice edge (15% concentration), respectively. SST anomalies in JJA 2023 in observations (D) and CESM2-NUDGE (E), and mean SLP and near-surface wind anomalies in JJA 2023 in ERA5 (F) and CESM2-NUDGE (G). Stacked bar-charts show the monthly time series of SIA anomaly (million km^2) for each Antarctic sector (defined in C) between 2016-01 and 2023-08 in observations (H) and CESM2-NUDGE (I). The black lines shows the total Antarctic SIA anomaly (million km^2).

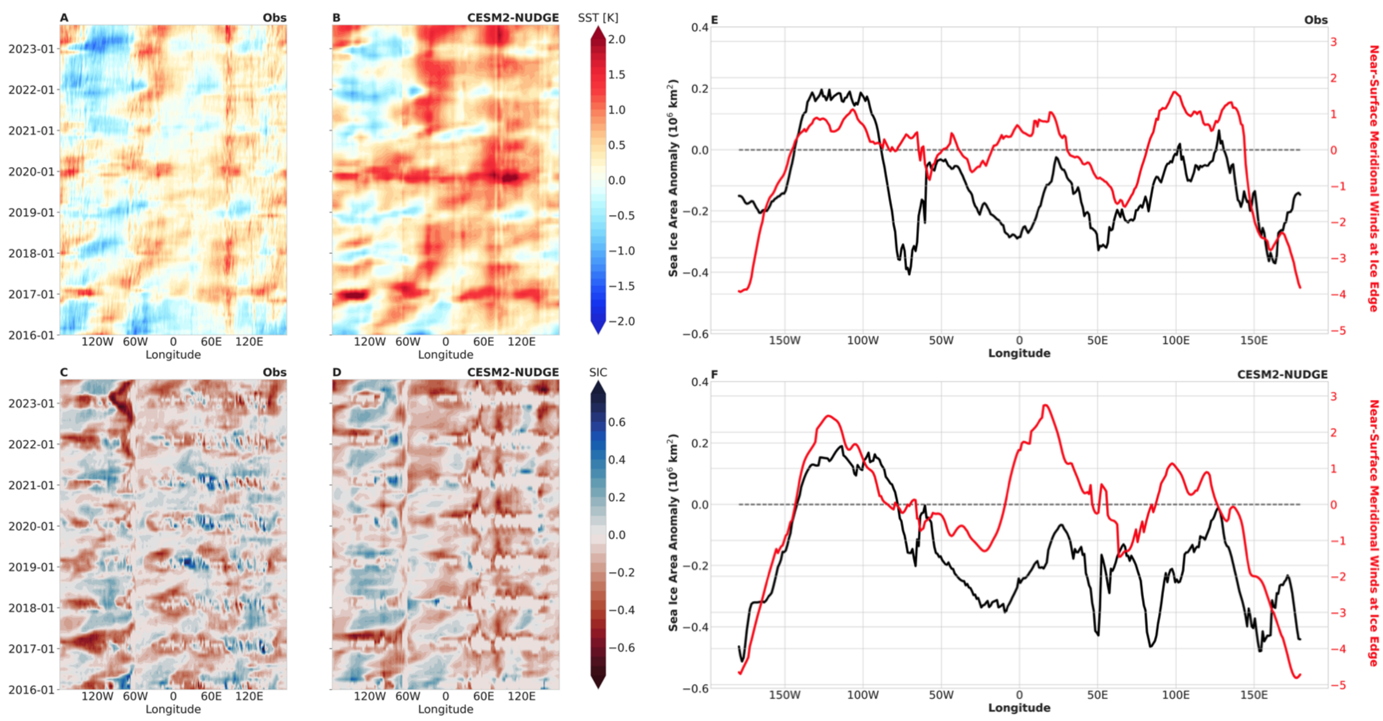

Figure 2. Monthly hovmoller diagrams of area-weighted SST anomalies (60°S-50°S) and SIC anomalies (within the climatological 1980-2020 sea ice 15% edge) in observations (A and C), and CESM2-NUDGE (B and D). Near-surface wind speeds at climatological sea ice edge and meridional-average sea ice area anomaly within climatological sea ice edge in JJA 2023 in ERA5 (E) and CESM2-NUDGE (F).

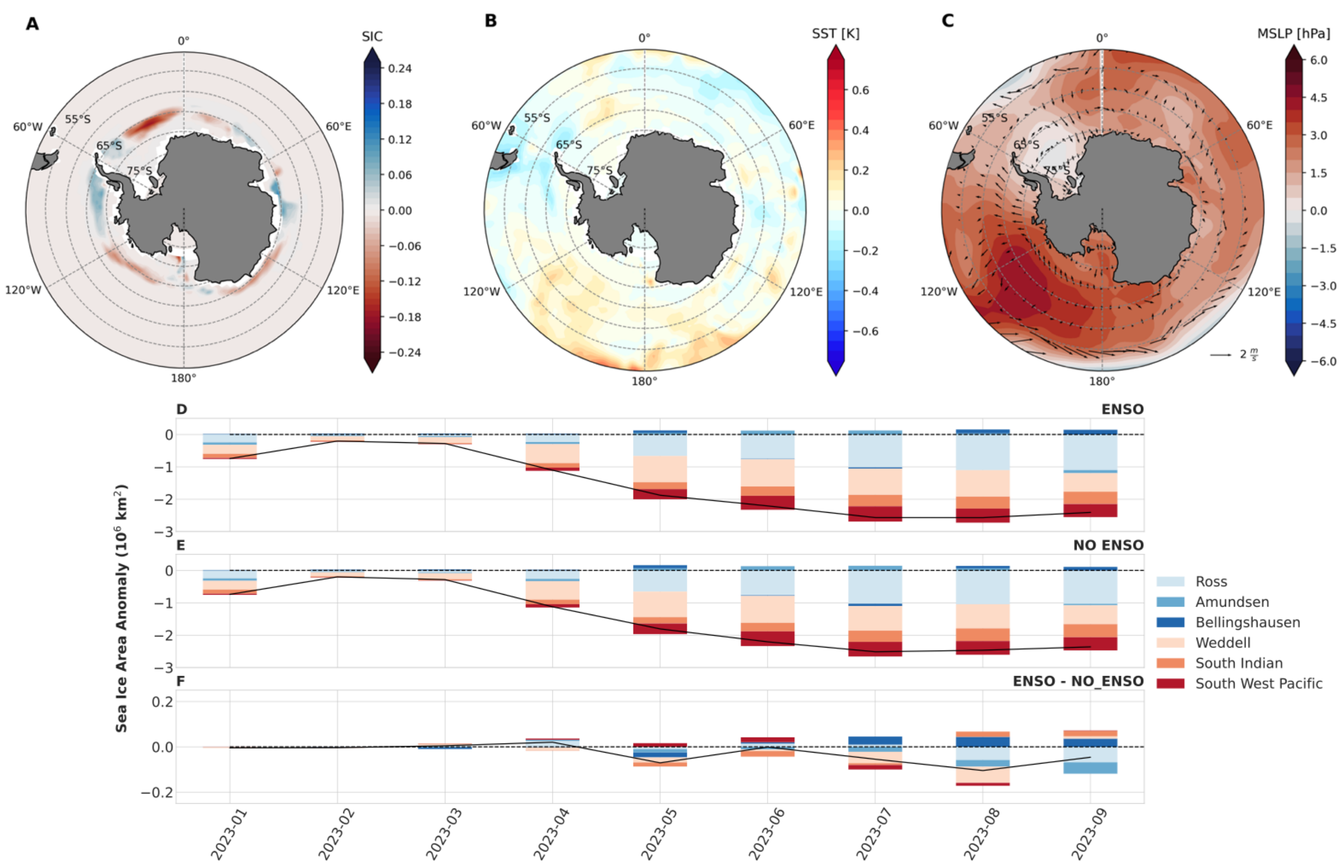

Figure 3. The difference in SIC anomalies (A), SST anomalies (B), and SLP and near-surface wind anomalies (C) between CESM2-NUDGE and CESM2-NO-ENSO-NUDGE in JJA 2023. Stacked bar-charts show the monthly time series of SIA anomaly (million km^2) for each Antarctic sector between 2023-01 and 2023-08 for CESM2-NUDGE (D), CESM2-NO-ENSO-NUDGE (E), and their difference (F).

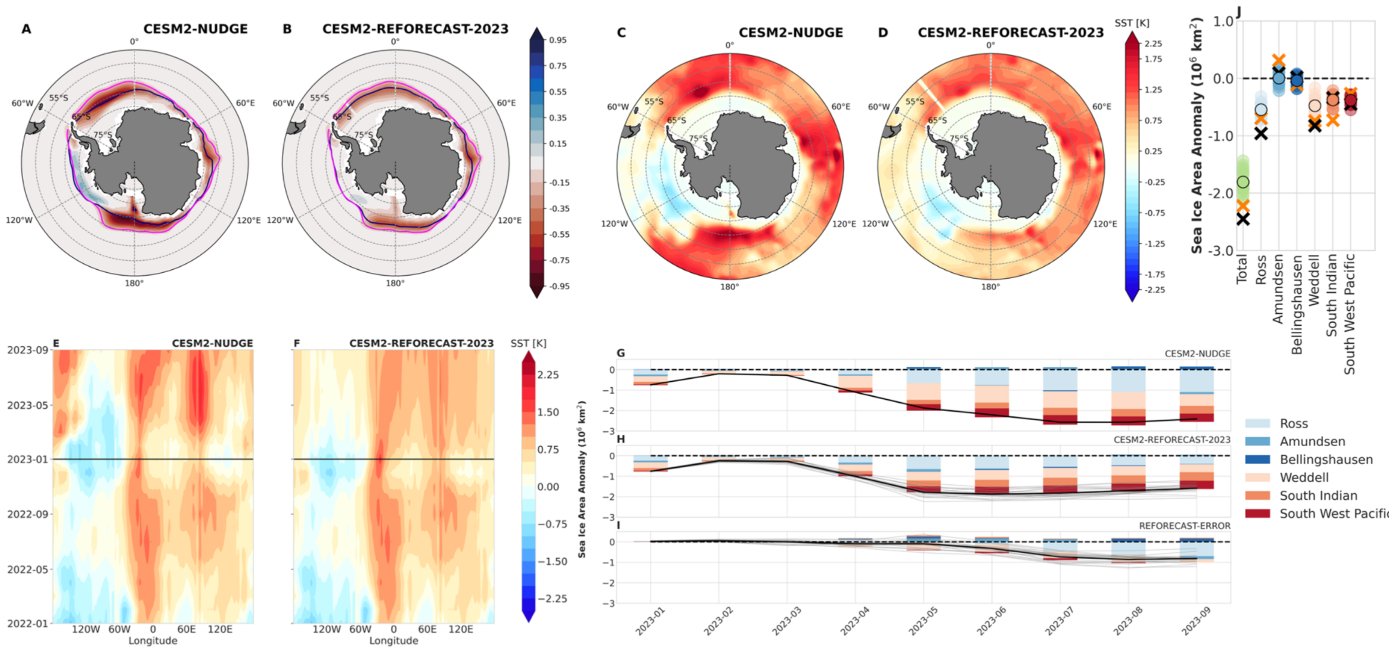

Figure 4. Mean SIC anomalies in June, July, and August (JJA) 2023 in CESM2-NUDGE (A) and CESM2-REFORECAST-2023 (B). Magenta and black contours indicate climatological average (1980-2020) and JJA 2023 sea ice edge (15% concentration), respectively. SST anomalies in JJA 2023 in CESM2-NUDGE (C) and CESM2-REFORECAST-2023 (D). Monthly hovmoller diagrams of SST anomalies (60°S-50°S) in CESM2-NUDGE (E), and CESM2-REFORECAST-2023 (F) between 2022-01 and 2023-08. Horizontal black line indicates the start time (2023-01) when CESM2-REFORECAST-2023 branches from CESM2-NUDGE. Stacked bar-charts show the monthly time series of SIA anomaly (million km^2) for each Antarctic sector between 2023-01 and 2023-08 for CESM2-NUDGE (G), CESM2-REFORECAST-2023 (H), and their difference (I) - interpreted as forecast error or the contribution of instantaneous atmospheric forcing. Regional SIA anomalies in JJA 2023 for each ensemble member in CESM2-REFORECAST-2023 (J)

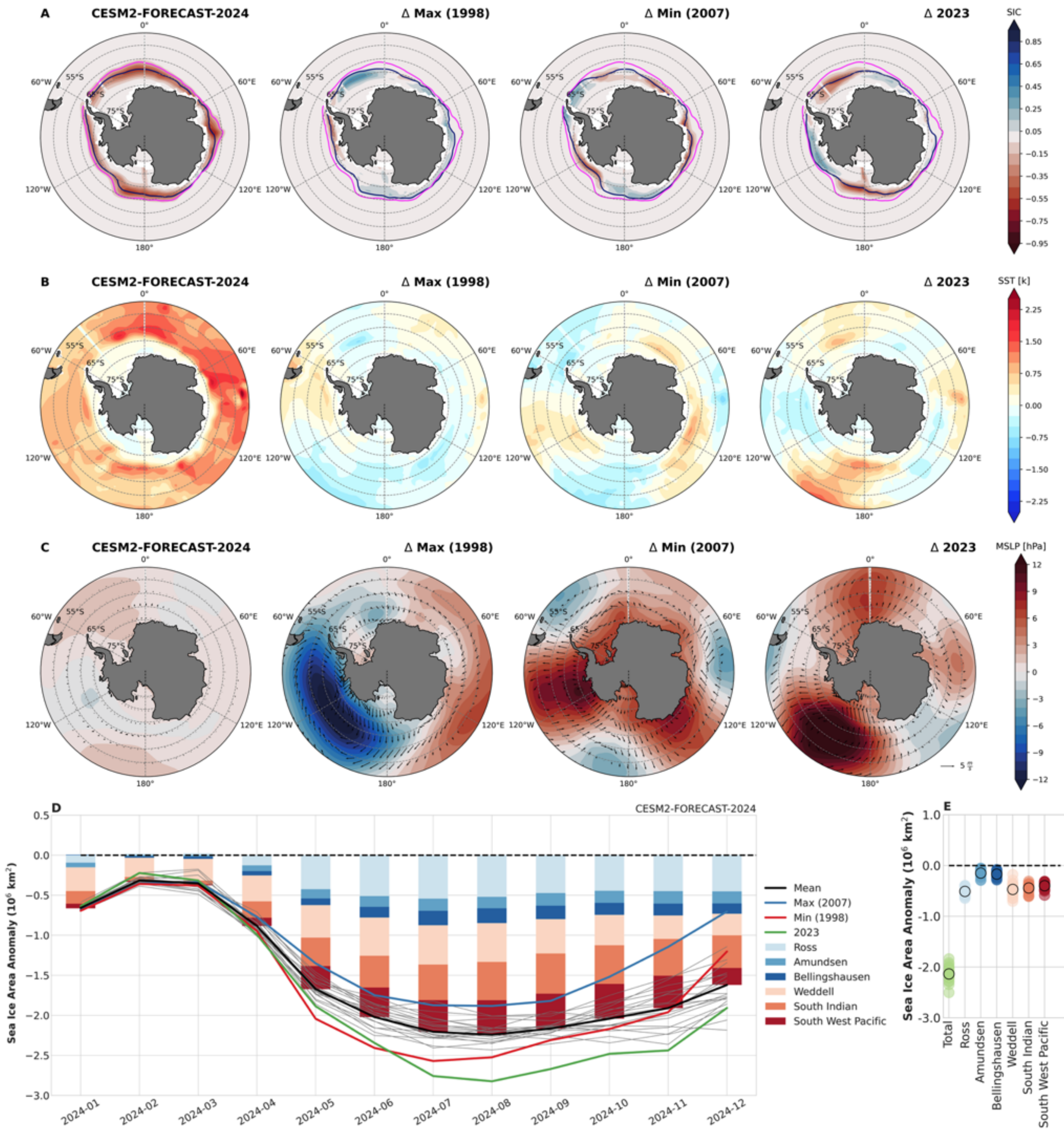

Figure 5. Ensemble-mean SIC (A), SST (B) and SLP and wind speed (C) anomalies in JJA 2024 from CESM2-FORECAST-2024. In top row, magenta and black contours indicate climatological average (1980-2020) and JJA 2024 sea ice edge (15% concentration). Remaining spatial panels show the the difference between the ensemble-mean and ensemble members nudged to winds from 1998 (ensemble member with maximum SIA in JJA 2024), 2007 (ensemble member with minimum SIA in JJA 2024) and 2023 (right column) for each spatial field. Timeseries of SIA anomalies from CESM2-FORECAST-2024 (D), and regional SIA anomalies in JJA 2024 for each each member in CESM2-FORECAST-2024 (E).